

# Piezoelectric Networks Obtained by Photopolymerization of Liquid Crystal Molecules

R. A. M. Hikmet

Philips Research Laboratories, P.O. Box 80.000, 5600JA Eindhoven, The Netherlands

Received March 30, 1992; Revised Manuscript Received June 23, 1992

**ABSTRACT:** A liquid crystal (LC) mixture containing reactive and nonreactive chiral molecules was made. The mixture showed the ferroelectric chiral smectic C phase with a spontaneous polarization of  $10 \text{ nC cm}^{-2}$  at  $80^\circ\text{C}$ . Upon photoinduced photopolymerization of the reactive molecules in the ferroelectric phase, a highly transparent oriented network with a dipolar orientation was produced. When such a film was subjected to periodic oscillations, a periodically varying open-circuit voltage across the sample could be detected, showing the piezoelectricity of the material. Using X-ray diffraction the origin of the piezoelectricity was related to the presence of chevrons and the tilted orientation of the molecules. The sign and the magnitude of the piezoelectric constant were largely dependent on the direction of the applied strain, and in the direction parallel to the molecular orientation it was found to be  $3.1 \text{ pC N}^{-1}$ .

## Introduction

Piezoelectricity of the polymers has long been known. The earliest work<sup>1</sup> on the subject dates back to 1924 and describes the piezoelectricity of various dielectrics. Since then many works have appeared in which the piezoelectricity in various polymers and the origin of the piezoelectricity in these systems are described.<sup>2</sup> It was found that, in addition to films, systems containing polar or nonpolar molecules could also show piezoelectricity. In the case of oriented films, the piezoelectric constant depended on the direction of applied strain with respect to the molecular orientation and showed a large variation in various samples. On the basis of various systems a theory was developed<sup>2</sup> to show that the piezoelectricity of polymers can be classified into four cases with regards to its origin: (i) the intrinsic piezoelectricity due to internal strain, i.e. displacement of atoms which is not affine to the average deformation of the system, (ii) the intrinsic piezoelectricity due to strain dependence of spontaneous polarization, (iii) the piezoelectricity originating from the polarization charge arising from strain-independent persistent polarization, (iv) the piezoelectricity from true changes embedded in the film. In cases iii and iv, heterogeneous strain must exist in the film. The polymers showing piezoelectricity were then broadly divided into three groups: (A) as-cast polymer films; (B) drawn polymers with intrinsic piezoelectricity; (C) polymers poled under a dc field (polymer electret). As-cast films (group A) show very weak piezoelectricity due to charges embedded in the film. These charges may be a true charge and/or polarization charge within the film. Group B polymers contain systems which have no symmetry center. During drawing, crystallites become oriented and/or liquid-crystal-like regions appear. Polymers belonging to this group show intrinsic piezoelectricity with an intermediate piezoelectric constant. Polymers belonging to group C, however, show the highest values of piezoelectric constant. The piezoelectricity of the polymers belonging to this group is largely due to the dipolar orientation within the system. The best-known polymer belonging to this group with the highest piezoelectric constant measured for a polymer is poly(vinylidene fluoride) (PVDF). PVDF in the  $\beta$ -crystal form is ferroelectric with a dipole moment perpendicular to the chain axis. PVDF polymer films are usually subjected to treatments in order to increase the  $\beta$ -crystal form, which include drawing and rolling. They are then poled under

very high electric fields in order to obtain films with high piezoelectricity.

Recently, piezoelectricity in liquid-crystal (LC) molecules in chiral nematic and smectic phases was predicted<sup>3</sup> and subsequently reported for LC elastomers.<sup>4,5</sup> LC molecules with reactive end groups were polymerized in solution to give multidomain lightly cross-linked LC systems (LC elastomers).<sup>6,7</sup> These multidomain samples without a dipolar orientation were subjected either to static<sup>5</sup> or periodically varying strain,<sup>4</sup> and open-circuit voltages across the samples were measured. Unfortunately, no value for the piezoelectric coefficient of these materials was reported.

Preceding the reports on elastomers, piezoelectricity in a chiral smectic C phase ( $\text{Sc}^*$ ) using low-mass LC molecules has also been observed.<sup>8</sup> In the  $\text{Sc}^*$  phase the LC director makes a tilt angle with respect to the smectic layer and this tilted orientation rotates about a helix. The special property of this phase is that the system possesses macroscopic electrical polarization without an external field, so it is classified as ferroelectric. LC polymers in the  $\text{Sc}^*$  phase, which has a monoclinic symmetry and a macroscopic molecular orientation in the unpoled state, can be categorized in group B. It is well-known that LC polymers and elastomers show phase transitions as the temperature of the system is changed, which can for example result in the destruction of the  $\text{Sc}^*$  phase. Furthermore, it is also known that poling can enhance the piezoelectricity of a polymer to a large extent (group C). Therefore, it can be desirable to have a temperature-stable poled polymer with a  $\text{Sc}^*$  structure.

Here I describe a novel anisotropic plasticized network with a dipolar orientation obtained by in situ photopolymerization of LC diacrylate containing nonreactive chiral molecules in the  $\text{Sc}^*$  phase under an electric field. Properties of anisotropic networks,<sup>9-11</sup> as well as gels and plasticized networks<sup>12,13</sup> obtained by polymerization in the nematic and chiral nematic ( $\text{N}^*$ ) phases, have been described. Here the optical properties of the LC molecules in the  $\text{N}^*$  and  $\text{Sc}^*$  phases before and after polymerization are described. Furthermore, the piezoelectric behavior of the system obtained by polymerization in the  $\text{Sc}^*$  phase and the influence of the smectic planes and the molecular orientation on piezoelectricity will be discussed.

## Experimental Section

Structure of the molecules used in the experiments are shown in Figure 1. C10 is a diacrylate prepared according to a previously

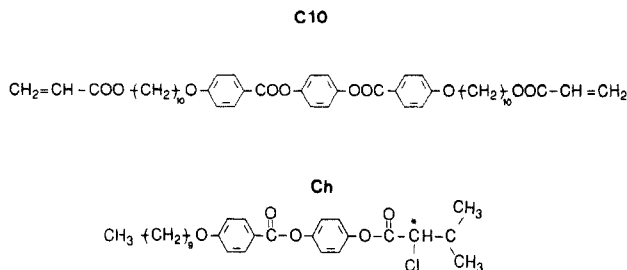


Figure 1. Structure of the molecules used.

**Table I**  
Transition Temperatures of C10 and the Chiral Mixture  
Used in the Present Study

C10 conc (% w/w)	transition $T$ (°C)					
	K	$S_c$	N	I		
100						
		82	108	149		
85	K	$S_c^*$	$N^*$	I		
		80	96	126		

published procedure.<sup>9</sup> The chiral dopant (Ch) was 4-[(*S*)-(+)-(2-chloro-3-methylbutyryl)oxy]phenyl 4-(decyloxy)benzoate (Aldrich Chemicals). The photoinitiator was Irgacure 651 (Ciba Geigy). Orientation of the molecules was obtained in cells provided with uniaxially rubbed Nylon orientation layers and transparent indium tin oxide electrodes. The thickness of the cell gap could be controlled to be between 2 and 60  $\mu\text{m}$  by varying the spacer thickness. Refractive index measurements were carried out using an Abbe refractometer which could be heated up to 140 °C. Dielectric measurements were carried out using a Hewlett-Packard 4194A Impedance/Gain-Phase analyzer. Dynamic mechanical thermoanalysis (DMTA) was performed using Polymer Laboratories DMTA equipment in the tensile mode. For the spontaneous polarization and the piezoelectric measurements a Keithley 617 electrometer was used. X-ray diffraction measurements were carried out using a Statton camera and Ni-filtered  $\text{Cu}_\alpha$  radiation.

## Results and Discussion

**Monomeric Mixture.** Induction of the  $S_c^*$  phase in systems showing the smectic C phase ( $S_c$ ) is usually done by the addition of chiral guest molecules with dipoles transverse to their long axes.<sup>14</sup> In order to obtain a polymerizable  $S_c^*$  mixture, C10 was doped with the chiral molecule shown in Figure 1. The transition temperatures of pure C10 in the monomeric state and a mixture containing 15% w/w of the chiral component are shown in Table I. As reported previously,<sup>11</sup> C10 in the monomeric state is crystalline at room temperature. At around 82 °C the material melts into the  $S_c$  phase. At around 108 °C it enters into a nematic phase (N) before becoming isotropic (I) at around 149 °C. The mixture containing the chiral dopant shows the  $S_c^*$  phase between 80 and 96 °C before becoming chiral nematic ( $N^*$ ) at 96 °C and isotropic at around 126 °C. It can be seen that the inclusion of the non-mesomorphic chiral dopant in C10 decreased the transition temperatures as it induced the  $S_c^*$  phase. Further on the text various properties of this mixture containing 85% w/w C10 (15% w/w chiral molecule) will be described.

Birefringence of the mixture in a uniaxially oriented state as a function of temperature is shown in Figure 2. Here it can be seen that in the  $N^*$  phase the birefringence decreases rapidly with increasing temperature, whereas in the  $S_c^*$  phase the birefringence remains almost unchanged. This is a typical behavior<sup>15</sup> observed for LC molecules and indicates that within the nematic phase the order parameter decreases much faster with increasing temperature.

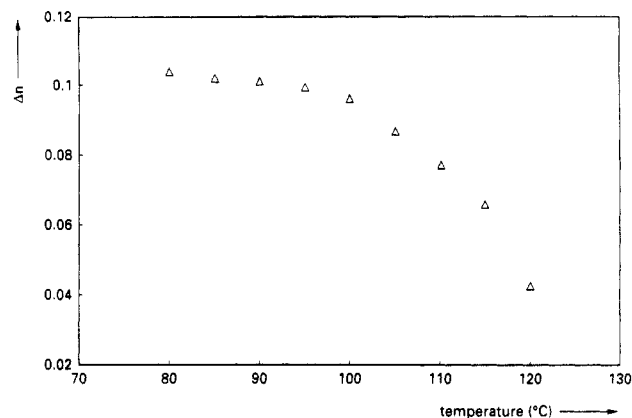


Figure 2. Birefringence as a function of temperature for the mixture (85% w/w C10) in the monomeric state.

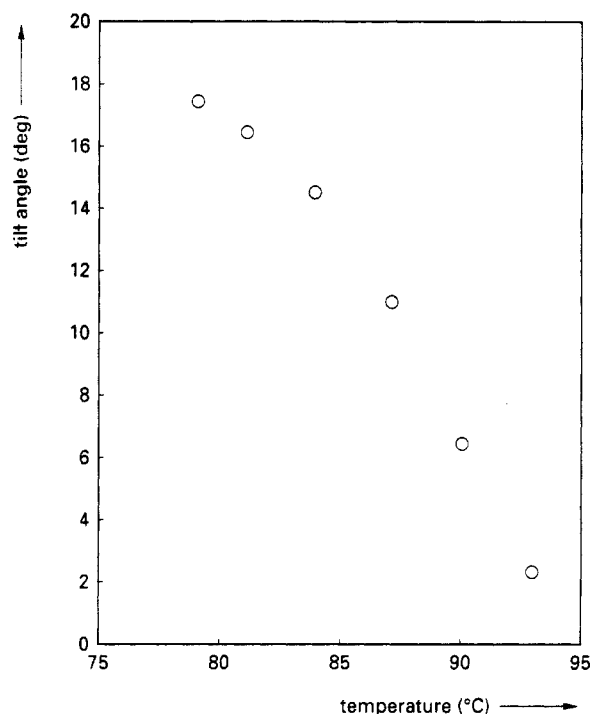
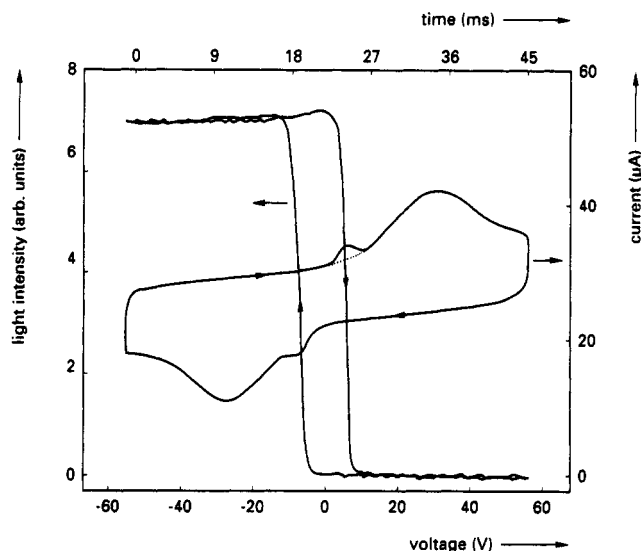
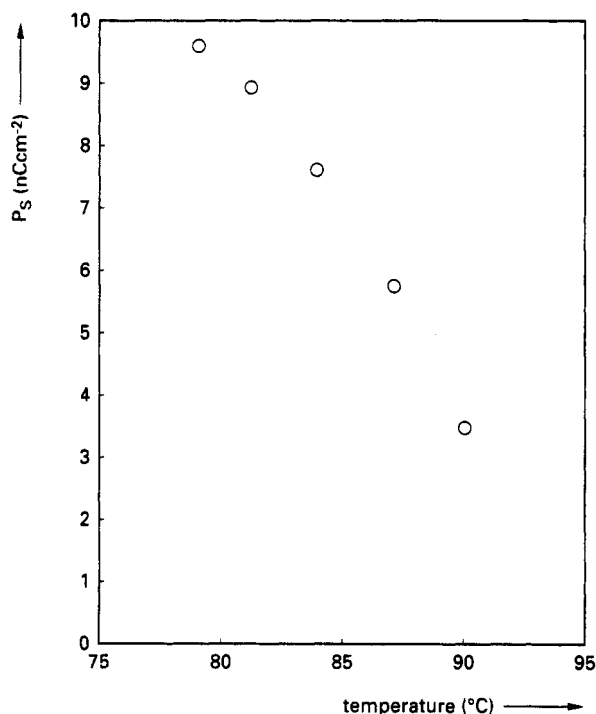


Figure 3. Tilt angle with the normal to the smectic layers as a function of temperature for the monomeric mixture.

The change in the tilt angle the molecules make with the smectic layer normal as a function of temperature can be seen in Figure 3. The tilt angle was estimated using an optical microscope by measuring the extinction angle as the direction of the applied field was reversed. This figure also shows a typical behavior for ferroelectric LC molecules where the cone angle decreases with increasing temperature. Furthermore, we measured the spontaneous polarization using the method described in ref 16. A triangular wave was applied across a cell containing electrodes, and the current through the sample was measured using the electrometer. Both the voltage and the current could be displayed on a digital storage oscilloscope and the traces plotted on an X-Y recorder. In Figure 4 the change in the current is shown as a function of voltage. A nonlinear behavior is quite apparent. In these cyclic curves two large current peaks, which change direction with the sign of the field, can be seen. In the first instance they were thought to be due to spontaneous polarization ( $P_s$ ) reversal. However on closer inspection, smaller peaks superimposed on the large peaks were seen. In order to find out which portion of the peak was due to the  $P_s$ , the transmission of light through the cell between crossed polarizers during the application of the electric field was followed. The light intensity through the cell as



**Figure 4.** Light intensity and the current through a cell containing the monomeric mixture as a function of cyclic voltage/time for the mixture at 80 °C,  $t = 90$  ms 110 V<sub>pp</sub>.



**Figure 5.** Spontaneous polarization of the monomeric mixture as a function of temperature.

a function of the voltage is also shown in Figure 4. The observed change in the light intensity is due to the change in the director orientation from being parallel to one of the polarizers to making a tilt angle, which causes an increase in the transmitted light intensity. In this process the direction of the  $P_s$  is also changed to give rise to a current pulse in the duration of reorientation. It can be seen that the change in the transmitted intensity occurs only in the duration of the small shoulder superimposed on the large peak. In order to calculate the  $P_s$ , the current peak was integrated over time and divided by the active area of the electrodes. In Figure 5 the  $P_s$  is plotted as a function of temperature. It can be seen that with increasing temperature  $P_s$  decreases, eventually vanishing at the clearing temperature showing a commonly observed behavior for the  $S_C^*$  phase, as also predicted by theoretical considerations.<sup>17</sup> Here it is important to point out that the origin of the large current peak is probably associated with the ionic impurities within the system and not with the spontaneous polarization. Indeed, when the area under

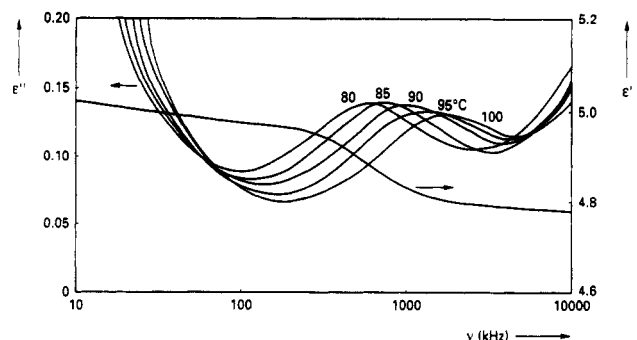


**Figure 6.** Dielectric constant and dielectric loss of the monomeric mixture measured at various temperatures.

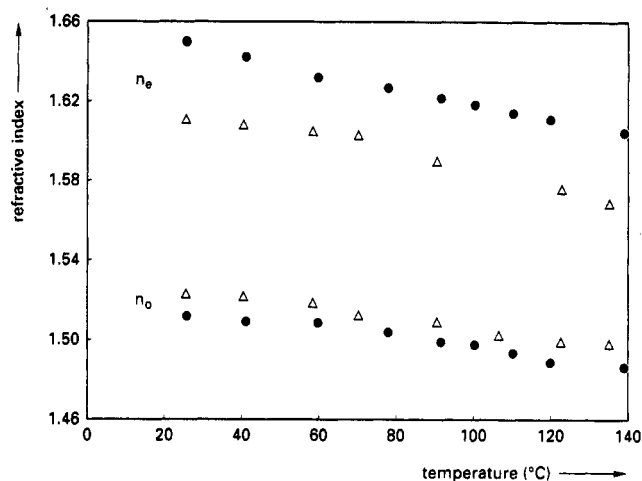


**Figure 7.** Refractive indices of uniaxially oriented plasticized networks obtained by polymerization of the monomeric mixture at (Δ) 115 °C and (●) 80 °C.

the large peak was measured as a function of temperature, a slight increase was detected. It is therefore easy to make a mistake and associate the large current peak with the spontaneous polarization if the director reorientation is not measured simultaneously. The characteristic of such a mistake is an increase in the  $P_s$  with increasing temperature.

Finally, using the mixture, the dielectric constant and the dielectric loss as a function of frequency in a cell where the orientation of the molecules was uniaxially planar were measured. The Goldstone model,<sup>18</sup> which corresponds to the fluctuations of the polarization vector at a constant tilt angle, was not measurable due to the existence of the ionic impurities, which probably also caused the large current peak in Figure 4. Therefore, 10-V bias voltage was applied across the cell, which immobilized the ionic impurities and enabled us to observe a peak in the dielectric loss curve. In Figure 6 the dielectric loss is plotted as a function of frequency at various temperatures together with the dielectric constant measured at 80 °C. It can be seen that the dielectric loss is very low and the peak frequency shifts toward higher frequencies as the magnitude of the peaks become smaller. Furthermore, the peaks persist even in the  $N^*$  phase. The relaxation peaks in the  $S_C^*$  phase are due to the soft mode<sup>18</sup> associated with the fluctuations in the tilt angle. The soft mode in the  $S_C^*$  phase transforms into another soft mode upon heating the system in  $N^*$ .

**Polymerized Networks.** Photopolymerization of the networks was carried out using a 100-W high-pressure mercury lamp (10 mW cm<sup>-2</sup> at 366 nm) after the induction of macroscopic orientation within the system. Upon polymerization highly transparent and birefringent networks were obtained. In Figure 7 refractive indices of the plasticized networks obtained by polymerization in  $S_C^*$

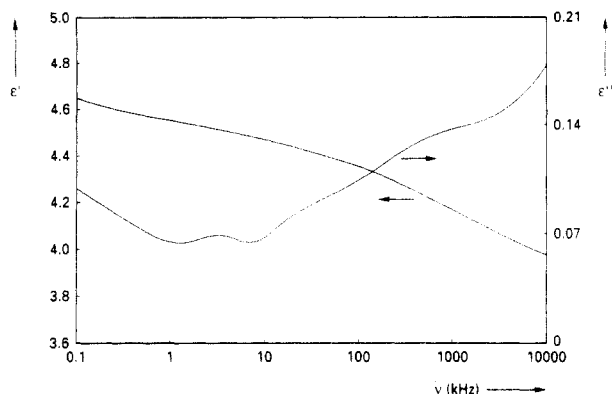


Figure 8. Dielectric constant and dielectric loss of the mixture polymerized at 80 °C measured at room temperature.

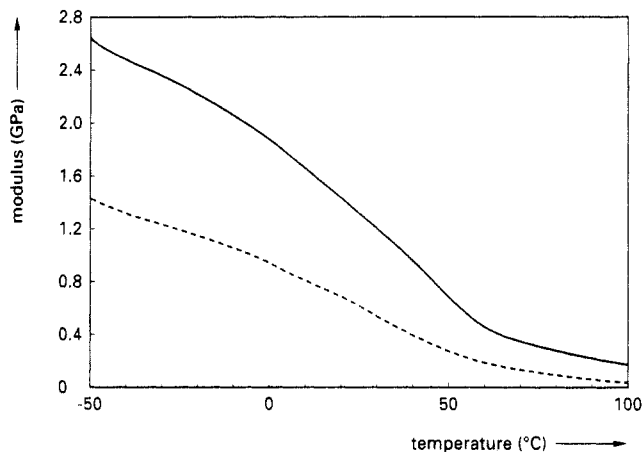


Figure 9. Tensile modulus of the mixture polymerized at 80 °C as a function of temperature measured in the direct (—) parallel and (---) perpendicular to the molecular orientation.

(80 °C) and N\* (115 °C) phases are plotted as a function of temperature. It can be seen that the polymer obtained in the  $S_C^*$  phase has a higher extraordinary refractive index ( $n_o$ ) than the polymer obtained in the N\* phase, whereas the ordinary refractive index ( $n_e$ ) shows the opposite behavior. When the birefringences of the systems are compared it can be seen that the polymer obtained in the  $S_C^*$  phase has a higher birefringence than the polymer obtained in the N\* phase. This behavior is associated with the order parameters and the birefringence of the molecules within the respective phases in the monomeric state, as indicated in Figure 2.

Dielectric constant and the dielectric loss of a uniaxially planar-oriented sample polymerized at 80 °C were measured as a function of frequency at room temperature, and the results are shown in Figure 8. It can be seen that while the form of the dielectric loss curve is changed considerably extent upon polymerization, only a small change in the form of the dielectric constant curve was observed. Furthermore, the magnitude of the dielectric constant at a given frequency showed a decrease upon polymerization. These effects can be associated with the reduced mobility within the system due to the polymerization of the C10 molecules and also a possible increased degree of association between the molecules.

Dynamic tensile moduli of the samples were measured at 1 Hz and 16- $\mu$ m peak-to-peak displacement using 8-mm-long samples. Results of the measurements in the direction parallel and perpendicular to the molecular orientation are shown in Figure 9. As reported previously<sup>19</sup> for other anisotropic networks, the sample in the present study also shows a very anisotropic behavior typical of oriented polymeric structures where values for the tensile modulus observed in the direction of molecular orientation are

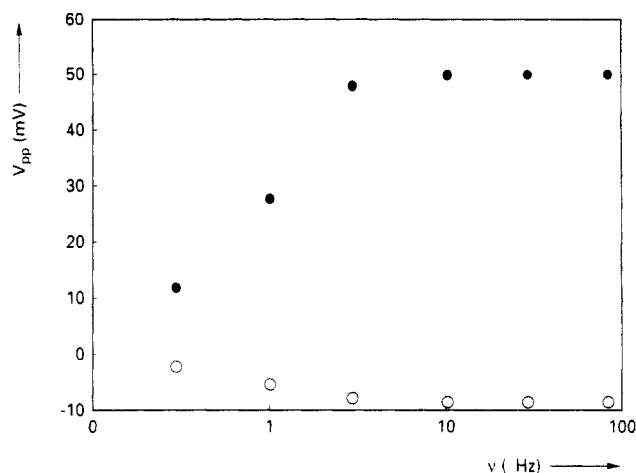
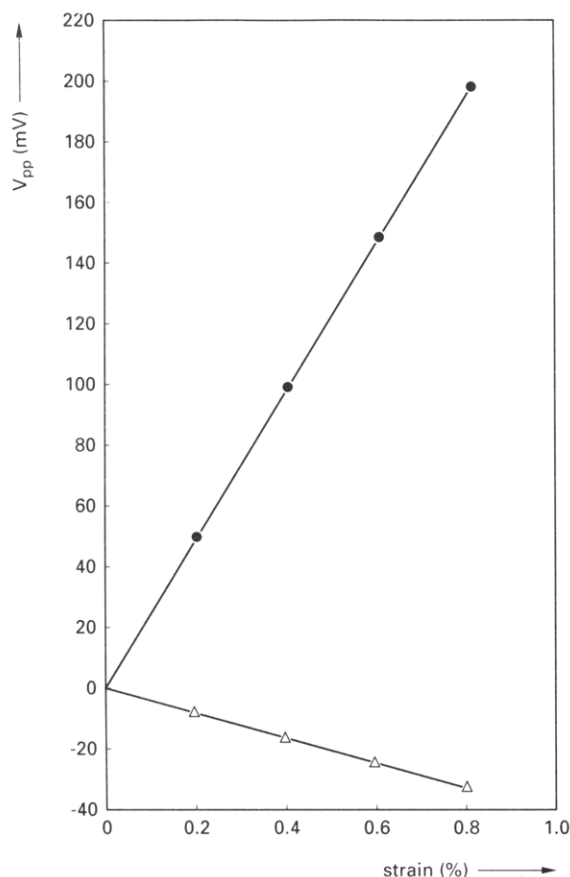


Figure 10. Peak-to-peak open-circuit voltage as a function of frequency for the mixture polymerized at 80 °C. Applied strain was in the direction (O) perpendicular and (●) parallel to the molecular orientation.

higher than in perpendicular directions.<sup>20</sup> In the direction of molecular orientation the number of load-bearing units is higher and they are oriented to a better extent compared with lateral directions, where the poorly oriented acrylate main chain bears the load explaining the observed anisotropy. However, the values observed here for the modulus in the direction of molecular orientation are very much lower than the values obtained for main-chain LC polymers. This difference was associated<sup>19</sup> with the conformational irregularities in the methylene groups of C10.

The open-field voltage across uniaxially oriented films provided with gold electrodes was measured by applying a sinusoidal strain in the direction parallel as well as perpendicular to the molecular orientation. The samples were 60  $\mu$ m thick and they were oriented under a dc field of 20 V. In Figure 10 the dependence of the peak-to-peak voltage measured at room temperature on the frequency of the applied strain is shown for two orientation directions. First, it can be seen that in the case of strain being in the direction of molecular orientation the open-circuit potential across the film is positive, the sign of the potential being defined by the direction of the electric field used in poling the sample. When the direction of the strain was changed to be in the direction perpendicular to the molecular orientation, it was found that the sign of the potential also reversed. This effect will be discussed further on in the text. The other effect to be seen in Figure 10 is the strong dependence of the open-field voltage on the frequency of the strain. This effect shows that the contribution to the piezoelectricity in the present case is to a large extent from the chiral molecules, which are not chemically attached to the network. From experimental as well as theoretical work<sup>17</sup> it is known that only the dipoles of the chiral molecules contribute to the spontaneous polarization in the  $S_C^*$  phase. In the present case polymerization in the  $S_C^*$  phase probably resulted in a structure where only the dipoles of the chiral molecules are oriented. Within the system, since the chiral molecules are highly mobile, their relaxation can take place at a fast rate (1 Hz). There is a contribution to this effect from the frequency dependence of the dielectric contribution. The fact that with decreasing frequency the open-field voltage tends to zero also shows that the main contribution to the piezoelectricity in the present case is due to relaxation of the chiral molecules in the network formed by C10. Furthermore, in order to estimate the piezoelectric constant ( $d$ ) in the directions parallel ( $d_x$ ) and perpendicular ( $d_y$ ) to the molecular orientation, the strain dependence



**Figure 11.** Peak-to-peak open-circuit voltage as a function of strain for the mixture polymerized at 80 °C. Applied strain was in the direction (Δ) perpendicular and (●) parallel to the molecular orientation.

of the peak-to-peak open-field voltage was measured at 10 Hz. The results for two different directions are shown in Figure 11, where the open-field voltage is plotted as a function of strain. It can be seen that the open-circuit voltage is a linear function of the applied strain. Values for  $d_z$  and  $d_y$  were calculated using the values for this figure together with the room-temperature tensile modulus and dielectric constant in the equation

$$d = V\epsilon_0\epsilon A_e / tE\gamma A_c \quad (1)$$

where  $V$  is the open-field voltage,  $\epsilon_0$  is the permittivity of the free space,  $\epsilon$  is the dielectric constant of the material,  $A_e$  is the active area of the electrode,  $t$  is the sample thickness,  $E$  is the tensile modulus in the direction of applied strain,  $\gamma$  is the strain, and  $A_c$  is the cross-sectional area of the sample. The piezoelectric coefficient in the direction of molecular orientation  $d_z$  was found to be 3.1 pC N<sup>-1</sup>, whereas in the direction perpendicular to the molecular orientation ( $P_y$ ) it was 1.4 pC N<sup>-1</sup>. The origin of this large difference is probably associated with the arrangement of the molecules within the films. Here it is important to point out that the 60-μm-thick samples used for the piezoelectric measurements were highly transparent. However, unlike 2-μm samples they did not make an angle with respect to the rubbing direction of orientation layers observable using optical microscopy.

In order to investigate the molecular packing which can give more information about the origin of piezoelectricity, X-ray diffraction was used. Diffraction patterns were recorded by setting the sample edge-on and flat-on to the horizontal X-ray beam, with flat surfaces of the samples in a vertical plane. The results are shown in Figure 12. In the flat-on case the presence of meridional small-angle peaks and equatorial wide-angle peaks is clear. This

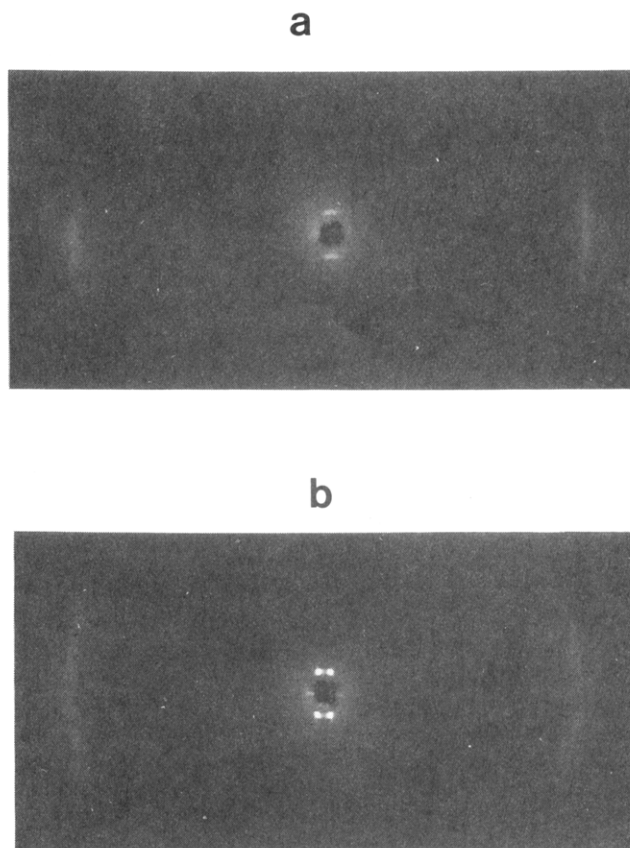


**Figure 12.** X-ray diffraction patterns of samples obtained by polymerized of the mixture at 80 °C: (a) flat-on; (b) edge-on to the horizontal X-ray beam, with flat surfaces of the samples in a vertical plane.

pattern indicates that there is a layer structure and the projection of these layers is perpendicular to the rubbing direction, and the long axis of the projected molecules makes a small angle with the layers. The picture becomes clearer when the edge-on pattern is considered (Figure 12b). It shows a four-point small-angle pattern and the splitting in the wide-angle arcs. This pattern indicates that there is a chevron structure and the long axis of the molecules makes a certain angle with respect to these layers. The existence of chevron formation during the cooling of low-mass LC molecules into the S<sub>C</sub>\* phase has already been demonstrated.<sup>21</sup>

A schematic representation of the layer structure and the angles defining the molecular orientation within the polymerized samples based on the S<sub>C</sub>\* phase is shown in Figure 13. In this schematic representation only a single chevron spanning the gap is shown for the sake of simplicity. The existence of several such chevrons along the gap cannot be ruled out. It can be shown that the angles  $\alpha$ ,  $\theta$ ,  $\delta$ , and  $\Omega$  are related to each other as  $\tan \Omega = \tan \omega \sin \alpha$  and  $\tan \alpha = (\cos \delta + \tan \Omega \sin \delta)(\tan \theta)/(\tan \omega)$ . In the case of molecules lying flat on the surfaces ( $\Omega = \delta$ ) the above relation is reduced to  $\cos \alpha = (\tan \theta)/(\cos \delta \tan \omega)$ . From X-ray diffraction patterns various angles were estimated to be  $\Omega = 6^\circ$ ,  $\delta = 16^\circ$  (from Figure 12b), and  $\theta = 8^\circ$  (from Figure 12a), showing that the molecules make an angle with respect to the flat surfaces. Using these values in the above equation, the tilt angle  $\omega$  was estimated to be  $10^\circ$ , which is considerably smaller than the value of  $18^\circ$  measured in the monomeric state (Figure 3). This indicates that during polymerization the tilt angle changes, causing reorganization of the system. However, the picture shown in Figure 13 still represents the layer structure and molecular orientation within the system. Assuming that the spontaneous polarization is not changed during

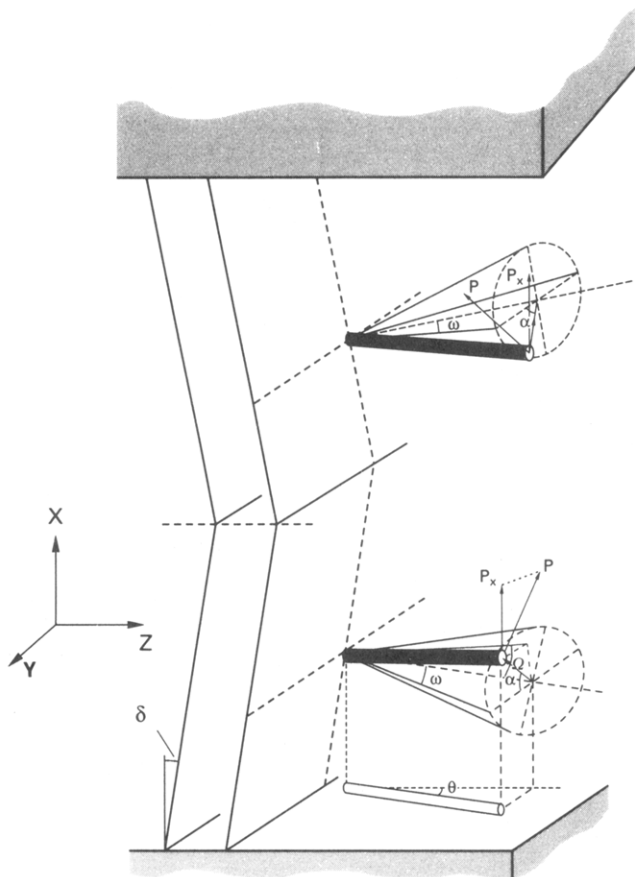


Figure 13. Schematic representation of smectic layer and molecular orientation within the samples.

polymerization, the  $x$  component ( $P_x$ ) of spontaneous polarization ( $P$ ) is given by

$$P_x = P \cos \alpha \cos \delta \quad (2)$$

For the present system  $P_x$  was calculated to be  $8 \text{ nC cm}^{-2}$ . Here it is interesting to compare the value for  $P_x$  and  $d$  obtained for the plasticized network in this study with the frequency quoted values of  $P = 13 \text{ } \mu\text{C cm}^{-2}$  and  $d = 28 \text{ pC N}^{-1}$  for  $\beta$  phase PVDF. It can be seen that even though the network has a much lower value for the spontaneous polarization, the difference in the piezoelectric coefficients is much smaller. This effect may be related to the presence of the chevron structure within the system and the orientation of the molecules within the chevrons, which may also provide an explanation for the change in the sign of the open-field voltage. In eq 2 it can be seen that  $P_x$  is dependent on angles  $\delta$  and  $\alpha$ . It can be envisaged that the effect of applied strain will be to orient the molecules in the direction of applied strain. This will probably involve rotation of the smectic planes around the  $z$  axis, i.e. a decrease in effective  $\alpha$ , hence an increase in  $P_x$ , explaining the observed behavior. In the case where the strain is applied perpendicular to the  $x-y$  plane, the smectic planes probably rotate around the  $z$  axis so as to increase  $\alpha$ , causing a decrease in  $P_x$ , thus explaining the sign of the open-circuit voltage. In both cases rotation of the planes around the  $x$  axis may also be expected. However, this rotation is not expected to cause any change in  $P_x$ .

## Conclusions

It has been shown that the LC diacrylate exhibiting a  $S_C$  phase can be doped with the chiral molecule to induce

the ferroelectric  $S_C^*$  phase. Upon doping, a decrease in the LC transition temperatures was observed. In the ferroelectric phase the polymerizable mixture showed the usual behavior, where the spontaneous polarization and the tilt angle the molecules makes with the normal to the smectic planes decreased with increasing temperature. The spontaneous polarization of the mixture and the tilt angle at  $80^\circ\text{C}$  were estimated to be  $10 \text{ nC cm}^{-2}$  and  $18^\circ$ , respectively. The mixture could be polymerized both in the  $S_C^*$  and  $N^*$  phases in order to obtain highly birefringent uniaxially oriented networks containing chiral molecules which were not chemically attached to the network. The networks obtained in the  $S_C^*$  phase had higher birefringence than the networks obtained by polymerization in the  $N^*$  phase. Networks obtained by polymerizing poled mixtures in the  $S_C^*$  showed piezoelectricity. The piezoelectric coefficient was found to be highly dependent on the direction of the applied strain. The values estimated for the piezoelectric constant for the strain in the direction parallel and perpendicular to the molecular are  $3.1$  and  $1.4 \text{ pC N}^{-1}$ , respectively. The change in the sign and the magnitude of the piezoelectric constant was related to the layered structure and the angle the molecules make with the surfaces. Finally, more work needs to be done in order to build a better understanding of the origin of the high values obtained for the piezoelectric constant for a system with a rather low spontaneous polarization. However, the ease with which these systems are produced and the prospect of using materials with higher spontaneous polarization and reactive groups make them a serious candidate for highly birefringent transparent piezoelectrics.

## References and Notes

- Brain, K. R. *Proc. Phys. Soc.* **1924**, *36*, 81.
- Hayakawa, R.; Wada, Y. *Advances in Polymer Science*; Springer-Verlag: Berlin, 1973, Vol. 11 (see also the references therein).
- Brand, H. R. *Makromol. Chem., Rapid Commun.* **1989**, *10*, 441.
- Vallerien, S. U.; Kremer, F.; Fischer, E. W.; Kapitza, H.; Zentel, R.; Poths, H. *Makromol. Chem., Rapid Commun.* **1990**, *11*, 593.
- Meier, W.; Finkelmann, H. *Makromol. Chem., Rapid Commun.* **1990**, *11*, 599.
- Finkelmann, H.; Kock, H.; Rehage, G. *Makromol. Chem., Rapid Commun.* **1981**, *2*, 317.
- Schatzele, J.; Kaufhold, W.; Finkelmann, H. *Makromol. Chem.* **1989**, *190*, 3269.
- Bonev, B.; Pisipati, V. G. K. M.; Petrov, A. G. *Liq. Cryst.* **1989**, *6* (1), 133.
- Broer, D. J.; Boven, J.; Mol, G. N.; Challa, G. *Makromol. Chem.* **1989**, *190*, 2255.
- Broer, D. J.; Hikmet, R. A. M.; Challa, G. *Makromol. Chem.* **1989**, *190*, 3202.
- Broer, D. J.; Mol, G. N.; Challa, G. *Makromol. Chem.* **1991**, *192*, 59.
- Hikmet, R. A. M. *Liq. Cryst.* **1991**, *9* (3), 405.
- Hikmet, R. A. M.; Zwerver, B. H. *Mol. Cryst. Liq. Cryst.* **1991**, *200*, 197.
- Simensmeyer, K.; Stegemeyer, H. *Liq. Cryst.* **1989**, *5*, 1187.
- Kelker, H.; Hatz, R. *Handbook of Liquid Crystals*; Verlag Chemie: Weinheim, 1980.
- Lee, J.; Chandani, A. D. L.; Itoh, K.; Ouchi, Y.; Takezoe, H.; Fukuda, A. *Jpn. J. Appl. Phys.* **1990**, *29* (6), 1122.
- Stegemeyer, H.; Meister, R.; Hoffmann, U.; Kuczynski, W. *Liq. Cryst.* **1991**, *10* (3), 295.
- Blin, R.; Žekš, B. *Phys. Rev. A* **1978**, *18*, 740.
- Hikmet, R. A. M.; Broer, D. J. *Polymer* **1991**, *32* (9), 1627.
- Ward, I. M. *Mechanical Properties of Solid Polymers*; Wiley Interscience: New York, 1983.
- Rikker, T. P.; Clark, N. A.; Smith, G. H.; Parmar, D. S.; Sirota, E. B.; Safinya, C. R. **1987**, *59* (23), 2658.

**Registry No.** C10, 125240-26-8; C10 (homopolymer), 132694-71-4; Ch, 109829-91-6.